

## Video Article

**Cardiac Muscle-cell Based Actuator and Self-stabilizing Biorobot - PART 1**Merrel T. Holley\*<sup>1</sup>, Neerajha Nagarajan\*<sup>2</sup>, Christian Danielson<sup>1</sup>, Pinar Zorlutuna\*<sup>2</sup>, Kidong Park\*<sup>1</sup><sup>1</sup>Division of Electrical and Computer Engineering, Louisiana State University<sup>2</sup>Department of Aerospace and Mechanical Engineering, Bioengineering Graduate Program, University of Notre Dame

\*These authors contributed equally

Correspondence to: Pinar Zorlutuna at [Pinar.Zorlutuna.1@nd.edu](mailto:Pinar.Zorlutuna.1@nd.edu), Kidong Park at [kidongp@lsu.edu](mailto:kidongp@lsu.edu)URL: <https://www.jove.com/video/55642>DOI: [doi:10.3791/55642](https://doi.org/10.3791/55642)

Keywords: Bioengineering, Issue 125, cardiomyocytes, biological actuator, biorobot, cell contraction, surface stress, cantilever

Date Published: 7/11/2017

Citation: Holley, M.T., Nagarajan, N., Danielson, C., Zorlutuna, P., Park, K. Cardiac Muscle-cell Based Actuator and Self-stabilizing Biorobot - PART 1. *J. Vis. Exp.* (125), e55642, doi:10.3791/55642 (2017).**Abstract**

Biological machines often referred to as biorobots, are living cell- or tissue-based devices that are powered solely by the contractile activity of living components. Due to their inherent advantages, biorobots are gaining interest as alternatives to traditional fully artificial robots. Various studies have focused on harnessing the power of biological actuators, but only recently studies have quantitatively characterized the performance of biorobots and studied their geometry to enhance functionality and efficiency. Here, we demonstrate the development of a self-stabilizing swimming biorobot that can maintain its pitch, depth, and roll without external intervention. The design and fabrication of the PDMS scaffold for the biological actuator and biorobot followed by the functionalization with fibronectin is described in this first part. In the second part of this two-part article, we detail the incorporation of cardiomyocytes and characterize the biological actuator and biorobot function. Both incorporate a base and tail (cantilever) which produce fin-based propulsion. The tail is constructed with soft lithography techniques using PDMS and laser engraving. After incorporating the tail with the device base, it is functionalized with a cell adhesive protein and seeded confluent with cardiomyocytes. The base of the biological actuator consists of a solid PDMS block with a central glass bead (acts as a weight). The base of the biorobot consists of two composite PDMS materials, Ni-PDMS and microballoon-PDMS (MB-PDMS). The nickel powder (in Ni-PDMS) allows magnetic control of the biorobot during cells seeding and stability during locomotion. Microballoons (in MB-PDMS) decrease the density of MB-PDMS, and enable the biorobot to float and swim steadily. The use of these two materials with different mass densities, enabled precise control over the weight distribution to ensure a positive restoration force at any angle of the biorobot. This technique produces a magnetically controlled self-stabilizing swimming biorobot.

**Video Link**The video component of this article can be found at <https://www.jove.com/video/55642/>**Introduction**

Biological actuators and biorobots are being actively studied to provide an alternative to conventional robotics for numerous applications. Biorobots that walk<sup>5,6,7,8</sup>, swim<sup>1,2,3,4</sup>, pump<sup>9,10</sup>, or grip<sup>11,12,13</sup> have already been developed. Similarly, muscle cells can be incorporated into a 3D rolled PDMS structure<sup>14</sup>. Often, the biorobot backbones are fabricated using soft lithography techniques with materials such as hydrogels and PDMS (polydimethylsiloxane). These are attractive choices because of their flexibility, biocompatibility, and easily tunable stiffness. Living muscle cells are usually incorporated with these materials to provide force generation through contraction. Mammalian heart muscle cells (cardiomyocytes) and skeletal muscle cells have dominantly been used for actuation. Besides these two, insect muscle tissues have been used to operate biorobots at room temperature<sup>3</sup>. In this two-part study, cardiomyocytes were chosen because of their spontaneous contraction<sup>6</sup>.

Much of earlier research on biorobots was focused on developing the biological actuators while optimization of the biorobot architecture and the development of essential functionalities for the biorobots were largely neglected. Recently, a few reports demonstrated the implementation of different swimming modes which were inspired by propulsion modes found in nature. These methods incorporate PDMS films and muscle cells to mimic various natural propulsion methods. For instance, flagella-based propulsion<sup>1</sup>, biomimetic jellyfish propulsion<sup>2</sup>, bio-hybrid ray<sup>4</sup>, and thin film PDMS swimming devices<sup>13</sup> have been reported.

In this paper, we present the fabrication process of self-stabilizing swimming biorobots which can maintain immersion depth as well as pitch and roll. The biorobot has a solid base or body, which is propelled by a single cantilever with cardiomyocytes attached to its surface. The cardiomyocytes cause the cantilever to bend in a longitudinal direction when they contract. This form of swimming is classified as ostraciiform swimming. The ability to add additional functionalities on the base is a unique advantage of ostraciiform swimming. For instance, the base can be utilized to provide excess buoyancy to carry additional cargos or control circuitry for cardiomyocyte contraction.

Stability of the biorobot was often overlooked in previous studies of biorobots. In this study, we implemented self-stabilization by designing the base with different composite PDMS materials of varying mass densities. The biorobot thus exhibits resistance to external disturbances and maintains its submersion depth, pitch and roll, unaided. The first layer is microballoon PDMS (MB-PDMS), *i.e.* PDMS mixed with microballoons,

which lowers the density of the biorobot, enabling it to float in media. The second layer is the PDMS cantilever, and its thickness is tailored such that force generated by the cardiomyocytes can dramatically bend the cantilever from 45° to 90°. The bottom layer is nickel-PDMS (Ni-PDMS), *i.e.* PDMS mixed with nickel powder. This layer performs multiple functions. It is magnetic, and therefore allows the biorobot to be anchored at the bottom of the medium, during cell seeding, with a magnet. The nickel mixture is of higher density than the MB-PDMS and medium, and ensure an upright position of the biorobot while floating. The weight of this layer generates a restoring torque on the biorobot at any pitch and roll. Also, the volume ratio between the Ni-PDMS and the MB-PDMS maintains the submersion depth. The presented protocols would be highly useful to researchers interested in characterizing the beating force of muscle cells and tissues, as well as those who wish to build swimming biorobots.

The seeding of the functionalized biological actuator and biorobot devices, the mechanical and biochemical characterization of the cells, and the quantitative analysis of the device function are described in detail in Part 2 of this two-part article as well as in the recent work<sup>15</sup>.

## Protocol

### 1. Calculate Mass of PDMS and Additives

- Use the following equation to find the mass of PDMS needed for specific heights in the following procedures,  

$$M = \rho * V = \rho * \text{Height} * \text{Area} \quad (1)$$
 where 'Height' is the height of the layer, 'Area' is the area of a container that the PDMS will be cured in, 'ρ' is the density of the mixture and 'V' is the volume.  
 NOTE: Densities for height calculations are PDMS = 0.965 g/mL, Ni-PDMS = 1.639 g/mL, MB-PDMS = 0.648 g/mL.
- Use equation (1) to estimate the mass of PDMS needed, for a given container, to obtain a specific height (5 mm) for the base of the biological actuator. The resulting density of PDMS is 0.965 g/mL.  
 NOTE: The ratio is 10:1 base to curing agent by weight.  

$$M_{\text{base}} = \rho * V = \rho * V * \left(\frac{10}{11}\right) \quad (2)$$

$$M_{\text{curing agent}} = \rho * V = \rho * V * \left(\frac{1}{11}\right)$$
- Use equation (1) to find the mass of Ni-PDMS needed, for a given container, to obtain a specific height (1.5 mm) of the bottom base of the biorobot.  
 NOTE: The ratios are 1:1.88 (Nickel Powder to PDMS by weight) and 1:1.71:0.171 (Nickel Powder to PDMS Base to PDMS curing agent by weight). The resulting density of Ni-PDMS will be 1.639 g/mL.  

$$M_{\text{Nickel}} = \rho * V = \rho * V * \left(\frac{1}{2.88}\right) \quad (3)$$

$$M_{\text{base}} = \rho * V = \rho * V * \left(\frac{1.71}{2.88}\right)$$

$$M_{\text{curing agent}} = \rho * V = \rho * V * \left(\frac{0.171}{2.88}\right)$$
- Similarly, use equation (1) to find the mass of MB-PDMS needed, for a given container, to obtain a specific height (3.5 mm) of the top base of the biorobot.  
 NOTE: The ratios are 1:5 (microballoons to PDMS by weight) and 1:4.54:0.454 (microballoons to PDMS base to PDMS curing agent by weight). The resulting density of MB-PDMS will be 0.648 g/mL.  

$$M_{\text{Microballoon}} = \rho * V = \rho * V * \left(\frac{1}{6}\right) \quad (4)$$

$$M_{\text{base}} = \rho * V = \rho * V * \left(\frac{4.54}{6}\right)$$

$$M_{\text{curing agent}} = \rho * V = \rho * V * \left(\frac{0.454}{6}\right)$$
- Check the dynamic stability of the biorobot with the desired dimension and geometry using the analysis scripts; see the supplementary information, 'Biorobot\_dynamic\_stability.m' and 'CG\_CB\_calculation.m'.

### 2. Fabrication of Biological Actuators on a Stationary Base

NOTE: See Figure 1a.

- Spin-coat a thin film of PDMS (see Figure 1a-1 and a2). The thickness of the resulting PDMS film will be 25 μm.**
  - Place a silicon wafer on a photoresist spinner and flip the pump switch on to produce suction.  
 NOTE: The silicon wafer has a 4-inch diameter and 500 μm thickness.
  - Pour positive photoresist (*e.g.* S1808) onto the silicon wafer until the wafer is completely covered. Program the spinner to spin at 2,000 rpm for 20 s. Then, engage the spinner by pressing on the foot pedal. Turn off the suction after spinning.
  - Heat a hot plate up to 120 °C. Use wafer tweezers to pick up the silicon wafer from the spinner and place the silicon wafer directly on the hotplate. Cover the wafer with a shallow petri dish and bake for 10 min.  
 NOTE: An oven can be used to bake the wafer using the same temperature and duration. **Figure 1a-1** depicts this process.
  - Place a plastic container on a weighing scale and zero it out. Pour 6 g of PDMS base into the container and add 0.6 g of PDMS curing agent. Mix the PDMS thoroughly for 5 min.  
 NOTE: After mixing, the mixture should be confluent with bubbles.
  - Place the container of mixed PDMS into a vacuum chamber. Reduce the pressure of the vacuum chamber to 100 mbar and leave the container in the chamber for 30 min. Break the vacuum, and remove the container. Keep the container covered until use.
  - Place the silicon wafer with the baked photoresist layer on the spinner. Slowly pour the entire degassed PDMS mixture on the wafer.  
 NOTE: Pour slowly so that no new bubbles are introduced into the mixture.
  - Set the spinner to 1,200 rpm for 5 min. Turn on the spinner suction and engage the spinner. Turn off the suction after spinning.

NOTE: These settings result in a 25  $\mu\text{m}$  thick layer of PDMS.

8. Heat an oven to 40 °C. Use wafer tweezers to pick up the silicon wafer from the spinner, then place it in the oven. Bake the wafer overnight and then cool the wafer at room temperature.

NOTE: **Figure 1a-2** depicts this process.

## 2. Laser engraving of the thin-film PDMS layer.

1. Turn on the power switch of the laser engraver and its exhaust. Turn on the computer connected to the laser engraver. Open the laser engraver software.
2. Under the "File" option, open the biological actuator design file shown in Figure 2e.
  1. Press the "Settings" button. Click on "Blue" and change the power setting to 3% and speed to 4%. Click "Set". Click on "Black" and change the "Mode" to skip. Then click "Set". Do the same for "Red". Press the "Apply" button to finish the settings."
  2. Push the "Activate the Engraver" button at the top right.
3. Press the "Relocate" button to move the design into the center of the software's screen.
4. Press the "Focus View" button in the program and click on the edge of the biorobot on the screen. This will move the guiding laser dot of the laser engraver to the corresponding point.
5. Move the wafer manually with tweezers, so that the point on the wafer corresponding to the point clicked in 2.2.4 is directly under the guiding laser dot.
6. Press the "Start engraving the prior job" button to start the engraving process. Remove the wafer after the engraving is completed. Turn off all equipment.

NOTE: The "Start engraving the prior job" button is the large green triangle. Do not look directly at the engraving process as the laser can damage the eyes. **Figure 1a-3** depicts this process.

## 3. Preparation and fabrication of the biological actuator base.

1. Pour glass beads (3 mm diameter) into a 15 mL tube. Immerse the beads with 70% ethanol in DI water for 24 h. Remove the ethanol and fill the tube with DI water for 24 h. Pour out the DI water and place the tube on a hotplate at 50 °C to facilitate drying of the glass beads.
2. Add 3 g to the amount of PDMS found in equation (1) to account for the PDMS that will stick to container sides during pouring. Use equation (2) to find PDMS base and curing agent amounts.
3. Place a plastic container on a weighing scale and zero it out. Pour the amount of PDMS base found in step 2.3.2 into the container and zero it out. Then pour the amount of PDMS curing agent found in step 2.3.2 into the container.
4. Mix the PDMS thoroughly for 5 min.  
NOTE: PDMS is used at a ratio of 10:1 base to curing agent. The mixture should have many bubbles.
5. Place a container to be used for baking on a scale and zero out. Carefully pour out the correct amount of PDMS found in step 2.3.2 (and mixed in step 2.3.4) into the container. Drop cleaned glass beads throughout the PDMS mixture at regular intervals. Leave a minimum of 5 mm of space surrounding each bead for the biological actuator base.
6. Place the container into a vacuum chamber. Reduce the vacuum pressure to 100 mbar and turn off the vacuum pump. After 30 min, break the vacuum and remove the container. Keep covered until use.  
NOTE: The pressure in the chamber may rise slowly over time as the mixture degasses and the vacuum chamber leaks. If the pressure increases substantially over 100 mbar, turn on the vacuum pump to restore the pressure to 100 mbar.
7. Heat a hotplate to 40 °C. Carefully place the container of PDMS and the glass beads on the hot plate. Cover the container and bake overnight.

## 4. Biological actuator assembly.

NOTE: The following procedure can be done with the naked eye.

1. Cut cubes (5 mm x 5 mm x 5 mm) out of the bulk PDMS made in part 2.3 using a razor blade.  
NOTE: One bead should be in the center of each cube.
2. Clean all sides of each biological actuator base, to remove any contaminants on the base surfaces, by pressing the base into the tape and remove. Repeat for each side.
3. Redo steps 2.3.2 to 2.3.6 to make a small amount of liquid PDMS. Dip the tip of a needle into the liquid PDMS. Place a drop of the liquid PDMS on the engraved base area of the wafer patterned in step 2.2. Smear the droplet of PDMS so that it completely covers the 5 mm x 5 mm base area.  
NOTE: The base area is the middle square section in **Figure 2a**.
4. Use tweezers to place the cleaned cube from step 2.4.2 on the base area that is covered with liquid PDMS.
5. Repeat step 2.4.3 from "Place a drop of liquid PDMS" to the end and step 2.4.4 for each device that will be made.
6. Heat a hotplate to 40 °C. Carefully place the silicon wafer with the assemblies on the hot plate. Cover the wafer and bake overnight.  
NOTE: Keep the assemblies attached until use. **Figure 1a-4** depicts the final device.

## 3. Fabrication of Biorobots (Figure 1b)

### 1. Spin-coating and laser-engraving a thin PDMS film

1. Repeat all steps in 2.1 and 2.2 using a new silicon wafer. This will result in a silicon wafer with a thin film of PDMS and a thin film of the photoresist, which is engraved with a biorobot design.  
NOTE: While repeating step 2.2, use the biorobot design for laser engraving instead of the biological actuator design previously used. **Figures 1b-1** and **b-3** depicts these processes.

### 2. Preparation and fabrication of PDMS composites.

NOTE: The following procedure can be done with the naked eye.

1. Pour phenolic microballoons into a 50 mL tube until full. Fill the tube with 70% ethanol in DI-water and let it sit for 24 h. Pour out the ethanol, add DI water, and let it sit for 24 h. Pour out the DI water, and then place the tube on a hotplate at 50 °C to facilitate the drying of the microballoons before use.
  2. Use equation (1) with the MB-PDMS density and 3.5 mm height to find the volume of PDMS required. Add 3 g to the total amount, to account for the material that will remain in the container after pouring. Use equation (3) to find the PDMS base and curing agent amounts. Measure out the appropriate amount of PDMS base, curing agent, and microballoons using the scale.
  3. Use equation (1) with Ni-PDMS density and 1.5-mm height to find the volume of PDMS needed. Add 3 g to the total amount as in step 3.2.2. Use equation (2) to find the PDMS base and curing agent amounts. Measure out the appropriate amount of PDMS base, curing agent, and nickel powder using the scale.
  4. Mix each mixture of MB-PDMS and Ni-PDMS for 5 min. Carefully pour the correct amount of MB-PDMS and Ni-PDMS calculated in 3.2.2 and 3.2.3 into separate containers using a scale.  
NOTE: The mixtures should be thoroughly mixed by a metal or glass rod without scratching the bottom surface of the mixing container. The mixture will be confluent with bubbles.
  5. Place both containers into a vacuum chamber. Reduce its pressure to 100 mbar for 30 min. Break the vacuum and remove the containers. Keep covered until use.
  6. Heat a hotplate to 40 °C. Place containers with MB-PDMS and Ni-PDMS on the hot plate. Cover each container and bake overnight.  
NOTE: Store with a lid until use.
3. **Biorobot assembly.**
1. Cut biorobot bases of dimensions respective to each biorobot size from Ni-PDMS and MB-PDMS using a razor blade. See **Figure 2b-2d** for base designs.  
NOTE: The thicknesses of Ni-PDMS is 1.5 mm and that of MB-PDMS is 3.5 mm.
  2. Clean all sides of the biorobot bases to remove any contaminants on the surfaces, by pressing the base into the tape and removing. Repeat for each side.
  3. Turn on a corona discharger. Bring the tip of the corona discharger 1 cm above the Ni-PDMS base, which is placed on a metal plate with a cleanroom tissue in between. Move the tip around the base and continue for 15 s to treat the surface.  
NOTE: A discharge should occur between the corona discharger and the wafer. If it does not, bring the tip closer until a discharge occurs.
  4. Repeat step 3.3.3 to treat the surface of the base of a biorobot engraved in step 3.1 for the same duration. Use tweezers to place the Ni-PDMS treated side onto the treated side of the film. Let the device sit for 5 min.  
NOTE: This will strongly bond the two parts. See **Figure 1b4**.
  5. Use sharp tweezers to peel the biorobot cantilever from the wafer and place it on the bottom of the Ni-PDMS base. Use tweezers to remove the entire assembly from the wafer.  
NOTE: The cantilever will be attached to the Ni-PDMS base. **Figure 1b-5** and **b-6** depicts this.
  6. Place a small drop of uncured PDMS (10:1 base to curing agent) on the top of the MB-PDMS base. Use tweezers to place the side of the Ni-PDMS with the thin film PDMS on the MB-PDMS with the uncured PDMS. Place the assembly in a plastic petri dish, and then place this on a hotplate at 40 °C to cure overnight.  
NOTE: **Figure 1b-7** depicts the final device.

## 4. Functionalization of the Devices

NOTE: Below, we describe the process of preparing the devices for cell seeding.

1. Prepare the required materials: Fibronectin solution (50 µg/mL), Phosphate Buffer Saline solution (PBS), Dulbecco's Modified Eagle Medium (DMEM) supplemented with 10% Fetal Bovine Serum (FBS) and 1% Penicillin antibiotic (DMEM complete).
2. Place 100 µL of fibronectin solution into the center of a T-25 culture flask (bottom surface when the flask is sitting upright). Maintain separate flasks for each device.
3. Place the biorobot or the biological actuator facing down over the droplet of fibronectin solution. Ensure that the cantilever is unfolded and immersed within the droplet. Incubate at 37 °C for 30 min.
4. After the incubation, remove the fibronectin solution and wash with PBS twice.
5. Remove the PBS and fill the flask with 10 mL of DMEM. Incubate at 37 °C for 1 h to facilitate degassing of the PDMS. To submerge the biorobots in 10 mL of media, use a magnet to hold the device at the bottom of the flask. Place the flask with the samples in an ultrasonication bath for 5 min to remove the bubbles.  
NOTE: During the incubation period, air bubbles form on the PDMS surface, which is referred to as degassing here. The Ni-PDMS used in the biorobot assembly is magnetic. The biological actuator does not need a magnet because it will remain at the bottom of the flask due to the weight of the glass bead. The biorobot or the biological actuator assembly is now ready for seeding, which is explained in detail in part 2.

## Representative Results

The biological actuator and biorobot have very similar fabrication processes, as the biorobot is a natural extension of the biological actuator (**Figure 1**). The biological actuator was developed first to establish techniques required for the biorobot, to analyze the force generated by the cells, and to characterize the cell maturation mechanically and biochemically, both of which are described in detail in Part 2 of this two-part article as well as in our recently published work<sup>15</sup>.

The spring constant of the actuator was assessed and tuned for a large change in radius of curvature of the cantilever during full contraction of the cardiomyocyte sheet. Then, we designed the biorobot while giving special consideration to its stability, control during cell seeding, and ease of locomotion. Initially, a few designs were chosen, as shown in **Figure 2b-2d**, with different properties to assess which attributes contribute the most to the design requirements. Biorobots were designed and tested with short, long, and wide cantilevers, as well as with multiple cantilevers to test the effect of changes in the actuator on biorobot function. We also considered different sizes of the floating base. The geometry of the base was maintained as a triangle as it creates the asymmetry that would result in a directional movement.

The stability of the biorobot was a critical component in the design process. The top MB-PDMS layer was used to provide buoyancy to the device, while the bottom Ni-PDMS layer was used for stability and magnetic control. Owing to a higher density, the base layer made of nickel provides the biorobot the ability to keep itself upright and return to its original position after exposure to external disturbances; shown in **Figure 3**. The layer also provides sufficient weight to keep the device afloat at the appropriate level. In this study, we provide an alternate approach, to develop a biorobot, which focuses on varying the properties of the mechanical backbone to create a self-stabilizing structure. Unlike other biorobots in the literature, the biorobot developed here can maintain its own pitch, roll and immersion depth. These parameters can be tuned by varying the mixing ratios of each composite material and their volume. However, there is a limit to total thickness of each base within the device beyond which the stability is compromised.

The following equation can describe the height of the biorobots above the surface of the medium:

$$h = \frac{H_{Ni}(\rho_{medium} - \rho_{Ni}) + H_{Mb}(\rho_{medium} - \rho_{Mb})}{\rho_{medium}} \quad (5)$$

where  $H_{Ni}$ ,  $H_{Mb}$ ,  $\rho_{medium}$ ,  $\rho_{Mb}$ , and  $\rho_{Ni}$  are thickness of Ni-PDMS, thickness of MB-PDMS, density of the medium, density of MB-PDMS, and density of Ni-PDMS, respectively (See **Figure 3b**). The height of the biorobots is one critical factor that affects the maximum load it can carry and its stability. Additional weight loaded on the base will lower the biorobots into the media and a larger volume of the base will be submerged. The additional volume to be submerged has a density lower than that of the medium and produces extra buoyancy to lift the added weight. Hence, to increase the maximum carrying load we need to increase  $h$  as much as possible. Nevertheless, the stability of the biorobot will be decreased as  $h$  increases. For maximum stability, the center of weight of the base should be as low as possible. However, increasing  $h$  would place the center of weight of the biorobot close to or above the medium, destabilizing the biorobot. Hence, detailed analysis is required to optimize the stability and the maximum carrying load simultaneously before modifying the base structure of the biorobot.

To determine the right thickness of each composite layer, various mixing ratios were tested with Ni-PDMS, and MB-PDMS. The maximum and minimum densities that could easily be mixed were  $0.648 \text{ g/cm}^3$  for MB-PDMS and  $1.64 \text{ g/cm}^3$  for Ni-PDMS, as shown in **Figure 3a**. All biorobot heights were designed so that the restoring moment of a biorobot at any tilting angle would be strong enough to bring it back to the horizontal position. A triangular shape was used to reduce hydrodynamic drag. The final dimensions are shown in **Figure 3d**. Using a computer script, the stability was numerically analyzed and proven to have a strong restoring moment using the two-layered method, as shown in **Figure 3e**. See table of materials and supplementary information for the computer program used.

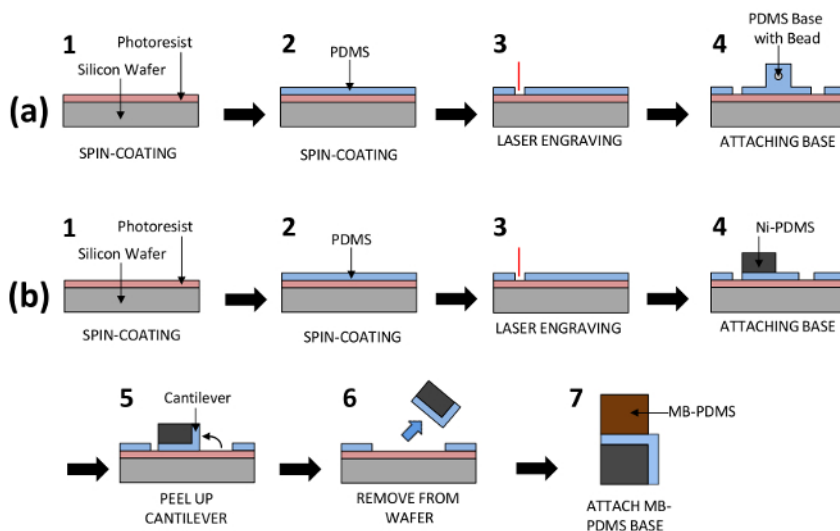


**Figure 1: Process Flow for the Fabrication of the Biological Actuator and Biorobot.** Each drawing represents the steps in the materials and methods in protocol sections 2 and 3 for biological actuator and biorobot fabrication. PDMS cantilevers are fabricated by spin-coating and laser engraving. Then the cantilevers are attached to a stationary base with a glass bead for the biological actuator (a) or to a self-stabilizing floating base for the biorobot (b). [Please click here to view a larger version of this figure.](#)

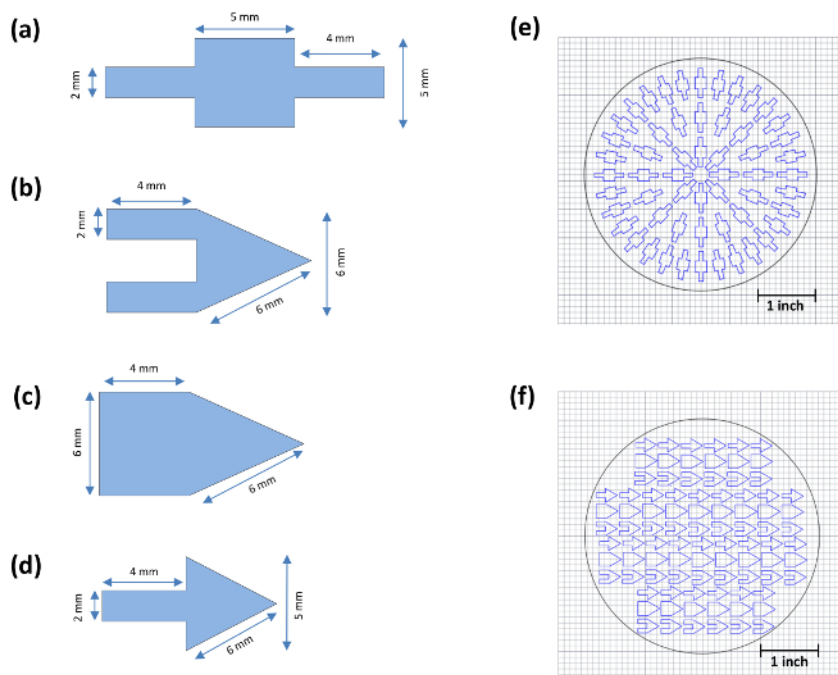


**Figure 2: Dimensions of the Biological Actuator and Biorobots that are Fabricated in this Study and the CAD Files for Engraving Both the Biological Actuator and Various Types of Biorobots.** (a) Biological actuator. (b) Double-arm cantilever biorobot. (c) Wide-arm cantilever biorobot. (d) Single-arm biorobot. (e) CAD drawing of biological actuator for laser engraving. (f) CAD drawing of biorobots for laser engraving. [Please click here to view a larger version of this figure.](#)

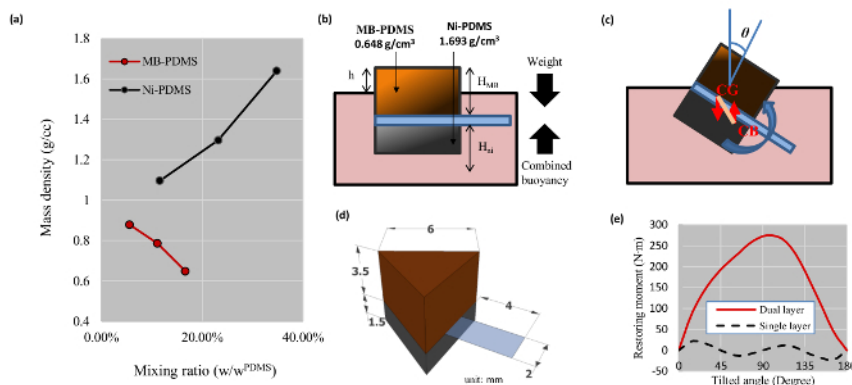


**Figure 3: Mixing Densities for Ni-PDMS and MB-PDMS and Stability of the Biorobots.** (a) Mixing ratios and resulting densities. (b) The densities and heights of the bases in relation to the media. (c) The rotation and restoration of the biorobot when tilted. The misalignment between the center of gravity (CG) and center of buoyancy (CB) generates a rotating moment. This moment will either restore the biorobot or cause it to tilt further. (d) The dimensions of the single arm biorobot in millimeter scale. (e) Restoring force was simulated for the single arm biorobot shown in part (c) under tilt conditions in (b) using two layers (Ni-PDMS and MB-PDMS) versus single layer (MB-PDMS). The graph shows that a single layer biorobot will not restore itself if it is tilted over 45°, whereas the dual layered biorobot will have always positive restoring force, keeping the biorobot upright. [Please click here to view a larger version of this figure.](#)

## Discussion

Various locomotion mechanisms can be found among aquatic swimmers<sup>16</sup>. The locomotion mechanism of the biorobot in this study uses fin-based locomotion, specifically ostraciiform locomotion. Ostraciiform swimmers propel themselves by wagging a tail (cantilever) and having a rigid body (layered base)<sup>16</sup>. Fish such as the boxfish and cowfish use this type of locomotion. Ostraciiform swimmers are typically slow and have inefficient body dimensions. Although ostraciiform swimming lacks velocity, this form of swimming allows engineers to implement various functionalities (such as dynamic stability) on the base or body. The biorobot design developed in this study is based on a solid base for floatation and stability, with a self-actuating cantilever as the propelling mechanism. One of the most important steps in the fabrication of the biorobot in this study is the thin film PDMS and laser engraving process to form the cantilever. Without a clean cantilever, the right mixture of PDMS (for elasticity), correct thickness (for spring constant) and dimensions (having sufficient area for confluent adhesion of cardiomyocytes to produce

motion), the biorobot will not operate. Moreover, it is also necessary to remove all bubbles from the cantilever surface through ultrasonication to create a viable surface for cardiomyocyte attachment.

The developed PDMS composite materials, MB-PDMS and Ni-PDMS can be used to precisely control the submersion depth and successfully produce the dynamic stability of the biorobots. The mass density of these materials can be finely tuned, as shown in **Figure 3a**. Furthermore, these materials do not show any negative effects on the maturation and contraction of the cardiomyocytes as we have shown in our recent work<sup>15</sup>. Hence, the developed materials can be widely used to implement a self-stabilizing and floating structure for biorobots and other applications.

Although the current protocol was able to build a self-stabilizing swimming biorobot, it has a few limitations. First, as the cantilever is manually peeled off from the wafer, the cantilever may be deformed during the process and the repeatability of the biorobot performance is affected. This can be addressed by using a water-dissolving sacrificial layer instead of the photoresist layer, so that the cantilever can easily be removed from the wafer; larger cantilevers can be used as well for higher power. Second, the procedure mainly relies on manual operations. The fabrication procedure can be streamlined for higher efficiency. For instance, the assembly process including the cardiomyocyte seeding can be modified so as to conduct it on a wafer level instead of individual device level. Lastly, the shape of the triangular base of the biorobot can be optimized to increase the directionality and stability of swimming.

Biorobots that harness the power generated by living muscle cells are of considerable interest as an alternative to traditional fully artificial robots. This protocol uses soft lithography and bio-MEMS techniques to produce a self-stabilizing, swimming biorobot. The particular design can be further refined. The efficiency of the actuator could be increased by patterning alignment cues for the cardiomyocytes on the cantilever surface. This will promote cell orientation and can increase the force generation of the cardiomyocytes<sup>17</sup>. The dimensions could also be varied or multiple cantilever arms could be attached, to further increase the net force from synchronized contractions. As described earlier, the multiple-layer base allows for tailoring of the height of the biorobot above the media surface. This determines the maximum carrying load and stability. Furthermore, we can substitute or add conductive materials to the cantilever in order to facilitate electrical stimulation. Electrical stimulation can be used to control the contraction rate of cells and the speed of the biorobots. We believe that the presented methods can be used to develop highly efficient biorobots for applications such as small package delivery.

## Disclosures

The authors have nothing to disclose

## Acknowledgements

M. T. Holley is supported by the Graduate Fellows program of the Louisiana Board of Regents and C. Danielson is supported by Howard Hughes Medical Institute Professors Program. This study is supported by NSF Grant No: 1530884. The authors would like to thank the support of the cleanroom at the Center for Advanced Microstructures and Devices (CAMD).

## References

1. Williams, B., Anand, S., Rajagopalan, J., Saif, M. A self-propelled biohybrid swimmer at low Reynolds number. *Nat Commun.* **5** (2014).
2. Nawroth, J., *et al.* A tissue-engineered jellyfish with biomimetic propulsion. *Nat Biotechnol.* **30**(8), 729-797 (2012).
3. Hugel, D. A swimming Robot Actuated by Living Muscle Tissue. *J Neuroeng. Rehabil.* **1** (2004).
4. Park, S., *et al.* Phototactic guidance of a tissue-engineered soft-robotic ray. *Science.* **353**(6295), 158-162 (2016).
5. Chan, V., Park, K., Colleens, M., Kong, H., Saif, T., Bashir, R. Development of miniaturized walking biological machines. *Sci. Rep.* **2**, 857 (2012).
6. Cvetkovic, C., *et al.* Three-dimensionally printed biological machines powered by skeletal muscle. *PNAS.* **111**, 10125-10130 (2014).
7. Xi, J., Schmidt, J., Montemagno, C. Self-assembled microdevices driven by muscle. *Nat. Mater.* **4**, 180-184 (2005).
8. Kim, J., *et al.* Establishment of a fabrication method for a long-term actuated hybrid cell robot. *Lab Chip.* **7**, 1504-1508 (2007).
9. Tanaka, Y., Sato, K., Shimizu, T., Yamato, M., Okano, T., Kitamori, T. A micro-spherical heart pump powered by cultured cardiomyocytes. *Lab Chip.* **7**, 207-212 (2007).
10. Park, J., *et al.* Micro pumping with cardiomyocyte-polymer hybrid. *Lab Chip.* **7**, 1367-1370 (2007).
11. Akiyama, Y., *et al.* Atmospheric-operable bioactuator powered by insect muscle packaged with medium. *Lab Chip.* **13**, 4870-4880 (2013).
12. Kabumoto, K., Hoshino, T., Akiyama, Y., Morishima, K. Voluntary movement controlled by the surface EMG signal for tissue-engineered skeletal muscle on a gripping tool. *Tissue Eng. Part A.* **19**, 1695-1703 (2013).
13. Feinberg, A., Feigel, A., Shevkopyas, S., Sheehy, S., Whitesides, G., Parker, K. Muscular thin films for building actuators and powering devices. *Science.* **317**(5843), 1366-1370 (2007).
14. Vannozzi, L., *et al.* Self-assembly of polydimethylsiloxane structures from 2D to 3D for bio-hybrid actuation. *Bioinspiration Biomimetics.* **10**(5), 056001 (2015).
15. Holley, M. T., Nagarajan, N., Danielson, C., Zorlutuna, P., Park, K. Development and characterization of muscle-based actuators for self-stabilizing swimming biorobots. *Lab Chip.* **16**, 3473-3484 (2016).
16. Sfakiotakis, M., Lane, D., Davies, J. Review of fish swimming modes for aquatic locomotion. *IEEE J. Oceanic Eng.* **24**, 237-252 (1999).
17. McCain, M., Agarwal, A., Hesmith, H., Nesmith, A., Parker, K. Micromolded gelatin hydrogels for extended culture of engineered cardiac tissues. *Biomaterials.* **35**(21), 5462-5471 (2014).